Inexpensive THz Focal Plane Array Imaging Using Miniature Neon Indicator Lamps as Detectors

Daniel Rozban, Assaf Levanon, Hezi Joseph, Avihai Akram, Amir Abramovich, Natan S. Kopeika, *Life Senior Member, IEEE*, Yitzhak Yitzhaky, Alexander Belenky, and Orly Yadid-Pecht

***Abstract*—Development of focal plane arrays (FPAs) for mm wavelength and THz radiation is presented in this paper. The FPA is based upon inexpensive neon indicator lamp Glow Discharge Detectors (GDDs) that serve as pixels in the FPA. It was shown in previous investigations that inexpensive neon indicator lamp GDDs are quite sensitive to mm wavelength and THz radiation. The diameters of GDD lamps are typically 3–6 mm and thus the FPA can be diffraction limited. Development of an FPA using such devices as detectors is advantageous since the costs of such a lamp is around 30–50 cents per lamp, and it is a room temperature detector sufficiently fast for video frame rates. Recently, a new 8 × 8 GDD FPA VLSI control board was designed, constructed, and experimentally tested. First, THz images using this GDD FPA are given in this paper. By moving around the 8 × 8 pixel board appropriately in the image plane, 32 × 32 pixel images are also obtained and shown here, with much improved image quality because of much reduced pixelization distortion.**

***Index Terms*—Detectors, far infrared, plasmas, terahertz (THz) imaging.**

I. Introduction

IMAGING systems in the electromagnetic spectrum between 100 GHz and 10 THz are required for applications in medicine, communications, homeland security, and space technology. This is because there is no known ionization hazard for biological tissue, and atmospheric attenuation of terahertz (THz) radiation is low compared to that of infrared and optical rays. The lack of inexpensive room temperature detectors and focal plane arrays (FPAs) in this spectral region makes it difficult to develop detection and imaging systems, especially real-time ones.

The Glow Discharge Detector (GDD) is a room temperature detector that is used in this study for direct THz radiation detection and imaging. There are several other room temperature THz detectors that are used for direct detection. The most popular detectors are Golay cells, pyroelectric, bolometers, and microbolometers, many of which are too slow for video frame rates. All are described in detail in [1]. Furthermore, there are THz cooled detectors which are very expensive [1]. The advantages of GDD are its low cost, its high responsivity, room temperature operation, and its relatively fast response.

A candidate for FPA pixels is miniature neon indicator lamps such as N523 of international light technology (Peabody, MA), which was tested experimentally and found to be a very good THz detector [2]. NEP is on the order of 10^{-9} W/Hz$^{1/2}$, and rise time is on the order of a microsecond. The mechanism of detection in such a Glow Discharge Detector (GDD) involves both enhanced ionization [3]–[8] and enhanced diffusion current [3], [4], [7], [9]–[11] caused by the incident THz wave. The former increases lamp current, while the latter decreases it. The dominant detection mechanism in such devices was found to be the enhanced ionization process leading to increase of lamp current. Detection mechanism effects have been studied in such devices and, indeed, incident THz electric field polarity has a noticeable effect on GDD responsivity [11] according to these opposing effects. In general, best response is obtained when the enhanced ionization is dominant. The lamp is ignited when internal dc bias breaks down the gas. As dc bias voltage may be 60–100 V and dc bias current may be several mA, the bias dc electric field in the lamps is quite high, especially since electrode separation is only about a millimeter or less. Light is emitted from the lamp because the high ionization and excitation collision rates between high kinetic energy free electrons and neutral gas atoms give rise to subsequent recombination and de-excitation. The incident THz electric field serves to increase free electron kinetic energy incrementally. However, this small increase in electron energy is sufficient to convert some inelastic collisions into ionization collisions, and some inelastic collisions into excitation collisions, in the latter case, ionization takes place with subsequent collisions with neutral atoms. In both cases, the GDD current is increased slightly by the incident THz electric field. The signal electrons generated in this manner are then accelerated too by the strong dc field, so that they too ionize neutral gas

Manuscript received November 28, 2010; revised January 06, 2011; accepted January 13, 2011. Date of publication January 24, 2011; date of current version July 29, 2011. The authors are grateful to the U.S. Office of Naval Research, the U.S. Army Night Vision and Electronic Sensors Directorate, and the Institute for Future Defense Technologies Research named for the Medvedi, Schwartzman, and Gensler Families, for their generous support, and to K. Krapels of NVESD for his kind expert advice and encouragement. The associate editor coordinating the review of this paper and approving it for publication was Dr. M. Abedin.

D. Rozban is with the Department of Electrical and Electronic Engineering, Ariel University Center of Samaria, Ariel 44837, Israel, and also the Department of Electro-Optical Engineering, Ben-Gurion University of the Negev, Beer-Sheva 84105, Israel (e-mail: rozbandaniel@gmail.com).

A. Levanon and A. Akram are with the Department of Electrical and Computer Engineering, Ben-Gurion University of the Negev, Beer-Sheva 84105, Israel (e-mail: levanonster@gmail.com; avihai21@gmail.com).

H. Joseph, N. S. Kopeika, Y. Yitzhaky, and A. Belenky are with the Department of Electro-Optical Engineering, Ben-Gurion University of the Negev, Beer-Sheva 84105, Israel (e-mail: josefy@ee.bgu.ac.il; kopeika@ee.bgu.ac.il; itzik@ee.bgu.ac.il; belenky@ee.bgu.ac.il).

A. Abramovich is with the Department of Electrical and Electronic Engineering, Ariel University Center of Samaria, Ariel 44837, Israel (e-mail: amir007@ariel.ac.il).

O. Yadid-Pecht is with the Department of Electro-Optical Engineering, Ben-Gurion University of the Negev (BGU), Beer-Sheva 84105, Israel. She is now on leave at the University of Calgary, Calgary, AB T2N 1N4, Canada (e-mail: orly.yp@gmail.com).

Digital Object Identifier 10.1109/JSEN.2011.2108282

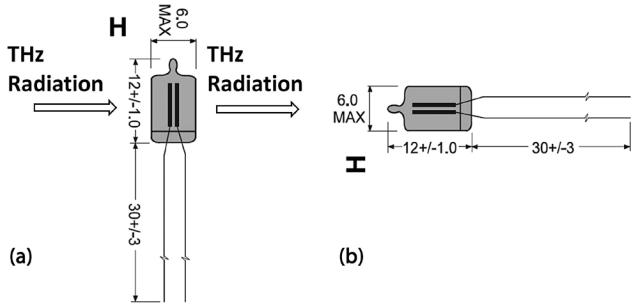

Fig. 1. Two configurations of GDD operation. (a) Side radiation. (b) Head-on radiation. Dimensions of GDD lamp N523 are in mm.

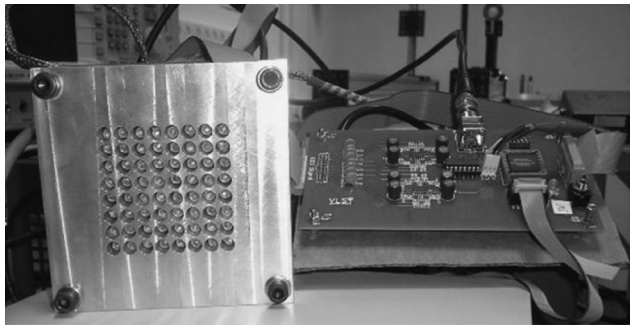

Fig. 2. A photo of 8 × 8 FPA with PCB board.

atoms in subsequent collisions, thus amplifying the signal current considerably. GDD plasma properties have been studied in three electrode lamps in which the third electrode is used as a Langmuir probe, and such internal avalanche amplification has been calculated to be on the order of six orders of magnitude [8]. Response by such devices is linear with incident electromagnetic wave power [2], [8]. This is important in imaging. In order to separate the detected THz signal from the large dc bias, it is desirable to modulate the intensity of the THz radiation, in which case the GDD acts as an envelope detector. A capacitor is then used to distinguish between the ac detected THz signal and the large dc bias.

Recent reports by others indicate GDD sensitivity at 200 GHz [12] is almost as good as that at 100 GHz [2]. Furthermore, imaging experiments in which a GDD is used in a scanning system indicate essentially no difference in image quality from that obtained using a Schottky diode detector instead [12]. However, success in developing less expensive real-time millimeter wave and THz imaging systems depends largely on the ability to develop inexpensive focal plane arrays. This paper focuses on the first focal plane array (FPA) using GDD detectors. Although the concept had been suggested previously [13], this is the first report of imaging results.

There are two configurations to realize an FPA with such lamps. The first is where the THz radiation is incident to the side of the lamp, and the second is where the radiation is incident head-on. Those two configurations are given in Fig. 1. In [2], NEP was measured for the side configuration in Fig. 1(a).

For relatively long range (far field) imaging, the effective pixel size is determined by

$$d = \frac{\lambda}{D} \cdot f \tag{1}$$

where d is the diffraction limited pixel diameter (which may be larger than the actual GDD diameter), λ is the THz radiation wavelength, f is the focal length of the quasi-optical system and D is the quasi-optic aperture. Using the head on configuration [see Fig. 1(b)] determines the diameter of the pixel in the array. Field-of-view (FOV) of the FPA is given by

$$\mathrm{FOV} = \frac{N\lambda}{D} \tag{2}$$

where N is the number of pixels in the FPA. The resolution of the FPA can be improved by minimizing FOV and pixel diameter.

II. Board

An 8 × 8 FPA based on GDD pixel, operating in head-on configuration with parabolic reflector for each GDD, was constructed in similar manner to the 4 × 4 GDD FPA [13]. A custom programmable board was designed and fabricated for an 8 × 8 GDD array. The board is used to connect together and synchronize an integrated operation of all elements of the system. The board is computer operated and permits different regimes of system operation. A photo of the 8 × 8 GDD FPA and PCB board is shown in Fig. 2.

The operation of the PCB board includes the following points.

- Interface to the GDD array.
- Amplification both in the pixel and in the column array levels.
- The signal recovery system.
- Multiplexing of rows and columns in a sequential manner.
- Sampling and digitization of the analog signals.
- Generate all necessary control clocks, voltage, and current references for the array and image display.
- Custom design software.

Interface to the GDD Array: The interface is a system for lighting any specific GDD by its address in the matrix, prefiltering, and reading out the analog signal. During the capturing, the GDDs are switched line by line in a rolling shutter mode. This method prevents the overheating of the matrix and gives the possibility to read out the analog signals from all the GDDs in one line.

Amplification in Pixel and Column Array Levels: The analog signal goes from the interface board to the preamplification stage. The amplified signal is translated through the commutation block to the signal recovery stage, for improving its signal-to-noise ratio (SNR).

The Signal Recovery System: The signal recovery system is based on a lock-in amplifier. The simplified model of a single GDD is shown in Fig. 3. As one can see, the noise is represented by two bulk noise sources: i_n is a bulk current noise, and e_n is a bulk voltage noise. $V_{\mathrm{ps\_rpl}}$ is ripple of the power supply, normally of low frequency, and can easily be filtered out by a high-pass filter. The dominant source of noise is shot noise of the bias current (i_n), although it can also be thermal noise according to electron heating temperature T_e, depending on bias current.

For this model, the SNR expression is

$$\mathrm{SNR} = \frac{\Delta IR}{\sqrt{\mathrm{BW}}\sqrt{e_n^2 + i_n^2 R^2}} \tag{3}$$

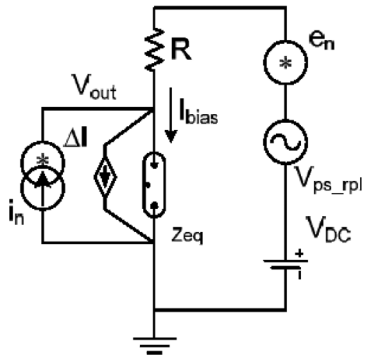

Fig. 3. The simplified equivalent circuit of the GDD with bias circuit and sources of noise. $V_{\mathrm{ps-rpl}}$ is ripple of the power supply, e_n is a bulk voltage noise source, i_n is bulk current noise source, Zeq is equivalent impedance of a GDD, and ΔI is response of the GDD to THz radiation (detected signal).

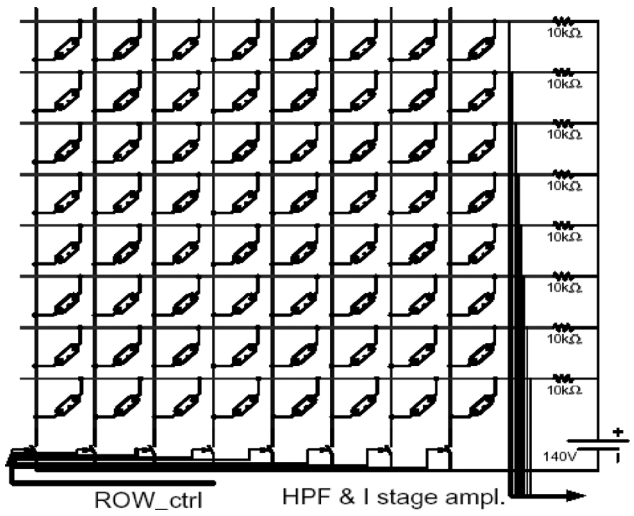

Fig. 4. The addressing circuitry for biasing, turning on the GDDs, and reading out the analog signal.

where ΔI is signal current, R is a bias resistor, and BW is electronic bandwidth. The experimental measurements that we performed have also brought us to conclude that shot noise is dominant at higher bias currents appropriate to THz wave detection. Thus, for BW of 1 MHz, I_{bias} is 7.5 mA, $i_n = 48\,\mathrm{nA/sqrt(Hz)}$, and $R||\mathrm{Zeq} = 2.2$ k. A typical detected signal of $\Delta I = 90$ pA produces an SNR of -40 dB. Since we prefer a good image at this stage, we aim for an SNR of 20 dB. Thus, SNR needs to be improved. A smart solution for the signal chain was designed and implemented. The designed system provides up to 100 dB signal recovery, while preserving a good tradeoff between the SNR and the frame rate.

Multiplexing in Rows and Columns in a Sequential Manner: The computer controlled system provides a very flexible read-out process. The preheating time, integration time, can be varied in dependence on the THz radiation power, distance of the source, noise level, etc. The scheme of the addressing circuit is depicted in Fig. 4.

Sampling and Digitization of the Analog Signals: The prefiltered and preamplified analog signal is converted into a digital one. From this point, all further signal processing can be done in a conventional way, using standard hardware/software.

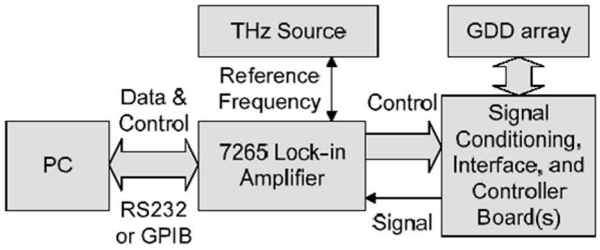

Fig. 5. The architecture of the system.

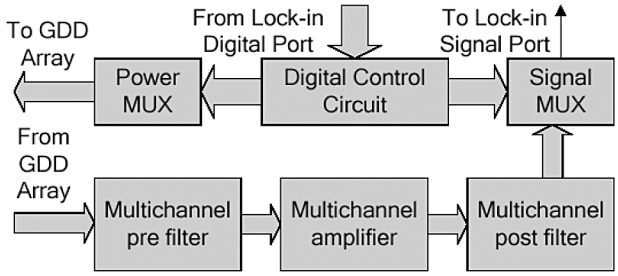

Fig. 6. The block diagram of the THz readout system.

The presented common column/row architecture has an intrinsic limit of channel isolation, consequently resulting in additional crosstalk among the elements. Careful circuit and board design was employed and led to a less than 10% crosstalk.

All Necessary Control Clocks, Voltage, and Current References for the Array and Image Display: Both power and signal multiplexers are controlled by a dedicated digital control circuitry, which is responsible for the overall system synchronization. The architecture of the system is depicted as a block diagram in Fig. 5.

Sequential readout of the pixels was utilized due to availability of only one lock-in amplifier. However, this approach has direct implication on the frame rate and limits further resolution increase. Consequently, in future systems, a parallel readout will be employed.

Custom Design Software: The software is intended to concentrate all the control in one computer. A user can control all parameters of the system. The user-friendly interface helps to get visualization of a picture from the sensor, to save the results in different ways, to run a capturing pixel-by-pixel, full image capturing, or sequence of frames as well. The software is ***lab-view*** compatible. The block diagram of the system is depicted in Fig. 6, and the sketch of the matrix is shown in Fig. 7.

The board is fully functional and working. Since GDD devices have never been applied to imaging previously, there is much to learn regarding possible non uniformity, fixed pattern noise, effects on detector linearity, noise, dynamic range, sensitivity to operating conditions, etc. All this is necessary before considering a larger array such as 32×32 one. Thus, our present step in imaging is an 8×8 focal plane array imaging using the current board. We will show implementation image processing on the 8×8 focal plane array images, and use the 8×8 pixel array to obtain images with 32×32 pixels.

In order to operate the GDD as THz detector, we have to provide about 100 V DC to break the gas down. Required dc bias is about 5 mA, thus yielding power consumption for a single

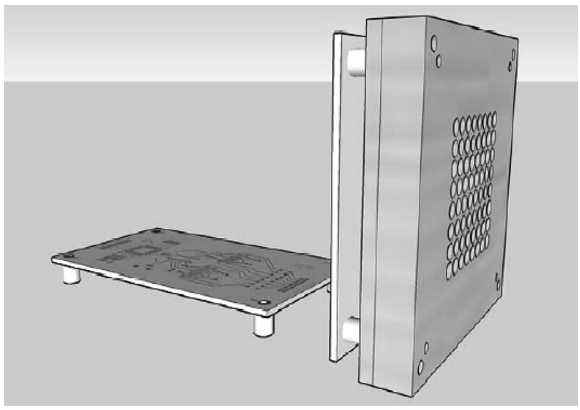

Fig. 7. The sketch of the matrix of GDDs, together with the interface board. The second board includes prefilters, preamps, MUXes, control circuitry, input/output connectors.

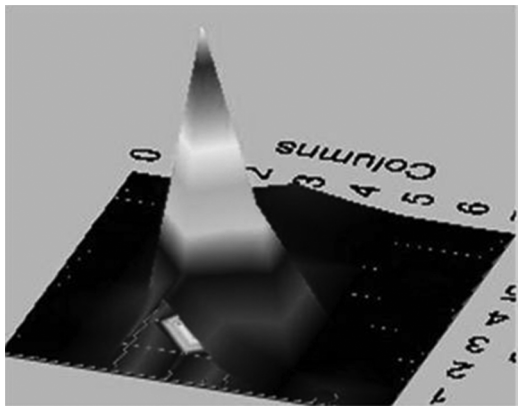

Fig. 8. THz image of 100 GHz focused beam imaged by the 8 × 8 FPA.

GDD about 0.5 watts. However, these devices can be used in a switching mode, whereby the GDD lamp can be switched on, detect a signal, read out, and switched off, all in less than a millisecond, thus reducing average power consumption by orders of magnitude.

III. Experimental SetUp and Imaging Results

A 100 GHz source was used to illuminate the object in this experimental setup. The 100 GHz source is based on GaAs multipliers of Virginia Diodes, Inc. (Charlottesville, VA, USA) that multiply a low-frequency source of 12.5 GHz 8 times to 100 GHz [14]–[16]. The 12.5 GHz signal was generated by an RF synthesizer and it was modulated by a 100 kHz reference signal from the PCB board of the FPA. The 100 GHz radiation was coupled out to free space by waveguide horn antenna. As preliminary testing of the 8 × 8 FPA and its PCB board we focused the 100 GHz beam with Polyethylene lens and placed the FPA in the focal plane. The image of the focused beam detected with the inexpensive 8 × 8 GDD FPA is shown in Fig. 8. It looks very similar to the image of a focused optical beam, but with a larger spatial scale according to larger wavelength and a "squarish" base according to the shape of the transmitter horn antenna.

In order to realize a THz imaging system proper quasi-optic components have to be developed. The quasi-optic design has

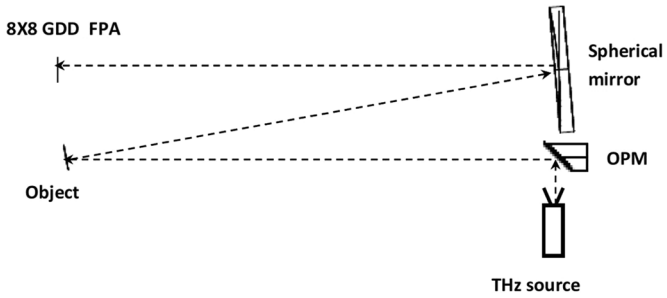

Fig. 9. Experimental setup of the imaging system.

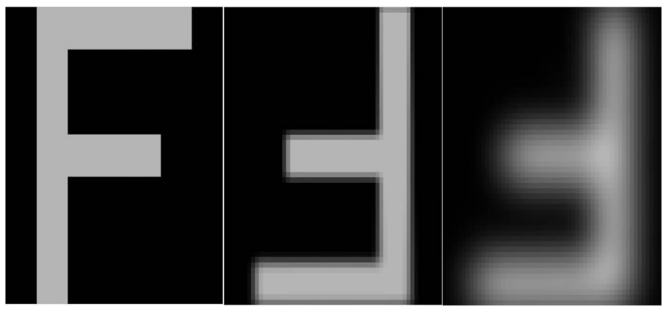

Fig. 10. Simulations of obtained "F" shape image in the quasi-optic system given in Fig. 9. Left: "F" shape object; middle: Geometrical aberrations; right: Diffraction effects.

to decrease the diffraction effects which are very dominant in the THz regime. This requires large aperture optical components. The design of the quasi optical setup was based on a 500 mm diameter spherical mirror with 1000 mm focal length as imaging mirror. The illumination of the object with collimated THz beam was performed by collimating Off-Axis Parabolic Mirror (OPM). The experimental setup of the imaging system is shown in Fig. 9.

The design of the quasi optic system was based on geometrical optics principles which states

$$\frac{1}{f} = \frac{1}{s_1} + \frac{1}{s_2} \tag{4}$$

where f is the focal length of the imaging objective, s_1 is the distance from the object to the imaging objective, and s_2 is the distance from imaging objective to the FPA. In order to enable imaging on the FPA we had to tilt the off-axis imaging mirror 5° as can be seen in Fig. 9. We used ZEMAX optical development software to optimize the system for minimum geometrical aberrations. In order to investigate the diffraction affects in the quasi-optical system of Fig. 9, a simulation of an "F" shape object was employed using ZEMAX software. The geometrical aberrations and diffraction effects in the obtained "F" shape image are given in Fig. 10.

A metal "F" shape object was placed in the object plane 2 m in front of the imaging mirror of the quasi-optical system shown in Fig. 9. This object was illuminated with a transmitted 150 mW+ collimated 100 GHz beam using the OPM. The 8 × 8 GDD FPA was placed 1.6 m from the imaging mirror to produce 1:0.7 imaging magnification (the size of the FPA is about 70× 70 mm, while the "F" object is 10 × 10 cm and the "F" height is about

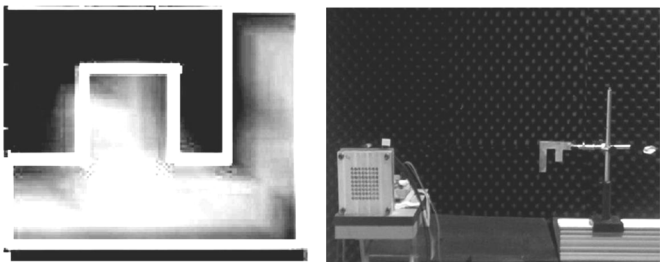

Fig. 11. THz image of a metal "F" shape object as was captured by the 8 × 8 GDD FPA (left); and the metal "F" shape object (right).

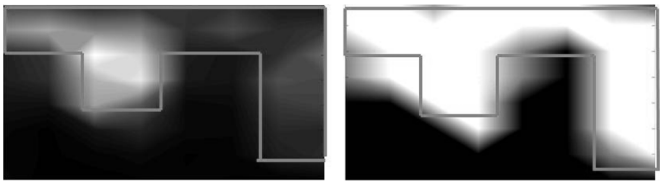

Fig. 12. THz images of "F" shape object: before using the correction algorithm (left) and after using the correction algorithm (right).

7 cm). Fig. 11 shows the "F" shape object and the image obtained in this case.

The "F" shape of the object is clearly seen in the image of Fig. 11 (with an outline of an ideal "F" shape superimposed over it). The intensity of the "F" image is not uniform due to the nonuniform illumination by the Gaussian beam illuminating the "F," as well as nonuniform GDD pixel response and electrical circuits. This is not unexpected since such devices are manufactured as inexpensive indicator lamps rather than as THz radiation detectors. For lower THz beam intensities, the obtained image degradation increases. Since the number of gray levels in THz images is limited, thresholding can be used to limit nonuniformity. Limiting nonuniformity was done using the following DSP algorithm: the readouts of the GDD pixels were divided into three levels; each level represents a different region of pixel readout, the three levels image is presented using MATLAB surface plot. Fig. 12 demonstrates this correction algorithm when a lower intensity THz beam illuminates the "F" shape object. For lower intensity illumination, the incident nonuniform Gaussian beam illumination is more apparent.

From Fig. 12, we can see that after employing the above DSP algorithm the "F" shape image can be observed easily. The blurring of the edges can be explained by diffraction effects and the low resolution of the current GDD array setup. The corrected image of Fig. 12 right is in good agreement with the simulation of Fig. 10. It is clear from Fig. 12 that reduced illumination intensity causes pixelization distortion to become more apparent.

Resolution Improvement: In order to improve resolution, we demonstrate operation of 32 × 32 GDD array by taking 16 different images with the 8 × 8 array, each at a different location in the image plane as can be seen in Fig. 13.

Using the same quasi-optic setup with imaging ratio of 2:1 magnification, 32 × 32 GDD pixel image of the "F" shape object were reconstructed from the sets of 16 images recorded with the 8 × 8 GDD FPA. Fig. 14 presents the reconstructed image of 32 × 32 pixels.

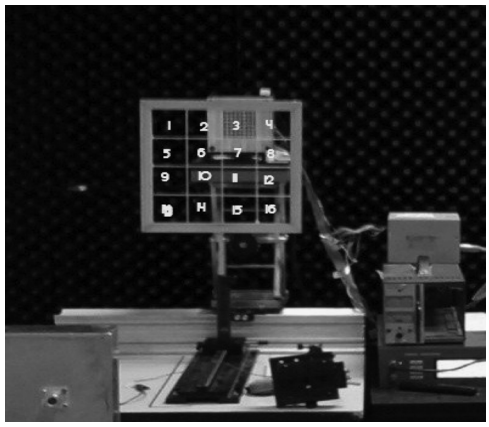

Fig. 13. Positions of 8 × 8 FFA in the 32 × 32 constructed image.

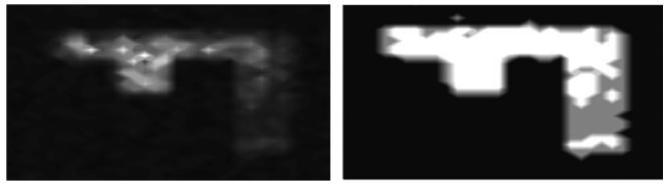

Fig. 14. 32 × 32 reconstructed THz images of "F" shape object: before employing the correction algorithm (left); and after employing the correction algorithm (right).

Fig. 15. 32 × 32 reconstructed image of a rotated "F" shape object: before employing the correction algorithm (left); and after employing the correction algorithm (right).

A 32 × 32 pixel image of a rotated "F" shape object was also obtained and is presented in Fig. 15. Clearly, the pixelization distortions in the 8 × 8 pixel images, as well as diffraction blur, are much reduced in the 32 × 32 pixel images of Figs. 14 and 15.

Dithering can help reduce speckle nonuniformity [17]. A 32 × 32 pixel board is presently being constructed.

IV. Conclusion

THz imaging using the 8 × 8 GDD FPA is presented here, which suggests that use of very inexpensive miniature gas discharge indicator lamps as detectors can greatly reduce the cost of millimeter wave and THz imaging systems, while still obtaining good image quality. The experimental results of the "F" shape images are in excellent agreement with simulation results of Fig. 10. The quasi-optical design and components prove themselves and minimize the diffraction effects in the images but with their limitations, as can be viewed in Figs. 11, 14, and Fig. 15. Reduction in illumination intensity makes pixelization and nonuniformities more apparent. The former can be dealt with by increasing the number of pixels, as shown in Figs. 14 and 15. The nonuniformities can be dealt with computationally. The quality of the 32 × 32 pixel images obtained using the 8× 8

pixel board encourages the development of higher resolution boards such as the 32 × 32 pixel system presently under construction. Dithering is planned for future systems.

Although it has been shown recently that plasmas can be used for mm wave imaging by recording the spatial and temporal variations in glow intensity as in the positive column for example [18], the electronic technique shown here seems to be much more sensitive while still retaining similar speed of response.

Future plans include investigating imaging via heterodyne detection [19]. The sensitivity improvement should obviate the need for a lock-in-amplifier in many applications.

REFERENCES

[1] F. Sizov, "THz radiation sensors," *Opto Electron. Rev.*, vol. 18, no. 1, pp. 10–36, 2010.

[2] A. Abramovich, N. S. Kopeika, D. Rozban, and E. Farber, "Inexpensive detector for terahertz imaging," *Appl. Opt.*, vol. 46, no. 29, pp. 7207–7211, Oct. 2007.

[3] M. A. Lampert and A. D. White, "Microwave techniques for studying discharges in gases," *Electron. Commun.*, vol. 30, pp. 124–128, Jun. 1953.

[4] B. J. Udelson, "Effect of microwave signals incident upon different regions of a dc hydrogen glow discharge," *J. Appl. Phys.*, vol. 28, pp. 380–381, Mar. 1959.

[5] P. J. W. Severin and A. G. Van Nie, "A simple and rugged wide-band gas discharge detector for millimeter waves," *IEEE Trans. Microw. Theory Tech.*, vol. MTT-14, pp. 431–436, Sep. 1966.

[6] N. H. Farhat, "Optimization of millimeter wave glow discharge detectors," *Proc. IEEE*, vol. 62, pp. 279–281, Feb. 1974.

[7] N. S. Kopeika, "On the mechanism of glow discharge detection of microwave and millimeter wave radiation," *Proc. IEEE*, vol. 63, pp. 981–982, Jun. 1975.

[8] N. S. Kopeika, "Glow discharge detection of long wavelength electromagnetic radiation: Cascade ionization process internal signal gain and temporal and spectral response properties," *IEEE Trans. Plasma Sci.*, vol. PS-6, pp. 139–157, Jun. 1978.

[9] G. D. Lobov, "Gas discharge detector of microwave oscillations," *Radiotekh Eleektron.*, vol. 5, pp. 152–165, 1960.

[10] D. Rozban, N. S. Kopeika, A. Abramovich, and E. Farber, "Terahertz detection mechanism of inexpensive sensitive glow discharge detectors," *J. Appl. Phys.*, vol. 103, pp. 093306-1–093306-4, May 2008, 1.

[11] A. Abramovich, N. S. Kopeika, and D. Rozban, "THz polarization effects on detection responsivity of Glow Discharge Detectors (GDD)," *IEEE Sensors J.*, vol. 9, pp. 1181–1184, Oct. 2009.

[12] L. Hou, H. Park, and X. C. Zhang, "Terahertz wave imaging system based on glow discharge detector," *IEEE J. Sel. Topics in Quantum Electronic*, vol. 17, no. 1, pp. 177–182, Jan.-Feb. 2011.

[13] A. Abramovich, N. S. Kopeika, and D. Rozban, "Design of diffraction limited focal plane arrays for mm wavelength and terahertz radiation using glow discharge detector pixels," *J. Appl. Phys.*, vol. 104, pp. 033302-1–033302-4, Aug. 2008.

[14] T. W. Crowe, J. L. Hesler, R. M. Weikle, and S. H. Jones, "GaAs devices and circuits for terahertz applications," *Infrared Phys. Technol.*, vol. 40, pp. 175–189, June 1999.

[15] J. A. Murphy and R. Padman, "Phase centers of horn antennas using Gaussian mode analysis," *IEEE Trans. Antennas Propagat.*, vol. 38, no. 8, pp. 1306–1310, Aug. 1990.

[16] P. F. Goldsmith, "Quasi optical technique at millimeter and sub-millimeter wavelengths," in *Infrared and Millimeter Waves*, K. Button, Ed. New York: Academic, 1982, vol. 6, ch. 5, pp. 277–343.

[17] K. Krapels, R. Driggers, R. Vollmerhausen, and C. Halford, "Performance comparison of rectangular (four point) and diagonal (two point) dither in undersampled infrared focal plane array imagers," *Appl. Opt.*, vol. 40, pp. 71–84, Jan. 1, 2001.

[18] M. S. Gitlin, V. V. Golovanov, A. G. Spivakov, A. I. Tsvetkov, and V. V. Zelenogorskly, "Time-resolved imaging of millimeter waves using visible continuum from the positive column of a Cs-Xe dc discharge," *J. Appl. Phys.*, vol. 107, pp. 063301-1–063301-11, Mar. 16, 2010.

[19] H. Joseph, N. S. Kopeika, A. Abramovich, A. Levanon, A. Akram, and D. Rozban, "Heterodyne detection by miniature neon indicator lamp glow discharge detectors," *IEEE Sensors J.*, in press.

Daniel Rozban received the B.Sc. degree in electronic engineering from the Ariel University Center of Samaria, Ariel, Israel, in 2006 and the M.Sc degree in electro-optic engineering from Ben-Gurion University of the Negev, Beer-Sheva, Israel, in 2009.

He is a Researcher in the Submillimeter Wave Laboratory, Department of Electrical and Electronic Engineering, Ariel University Center of Samaria.

Assaf Levanon, photograph and biography not available at the time of publication.

Hezi Joseph, photograph and biography not available at the time of publication.

Avihai Akram, photograph and biography not available at the time of publication.

Amir Abramovich received the B.Sc. and M.Sc. degrees in electrooptic engineering from Ben-Gurion University of the Negev, Beer-Sheva, Israel, in 1989 and 1991, respectively, and the Ph.D. degree from Tel-Aviv University, Tel-Aviv, Israel, in 2001.

He was with TAAS Israel Industries in the Counter Measures and Spectroscopic Characterization Department. He is a Researcher and Member of Staff in the Department of Electrical and Electronic Engineering, Ariel University Center of Samaria, Ariel, Israel. He is the Head of the Millimeter and Submillimeter Wave Laboratory. He has received research grants to develop and construct THz imaging system for homeland security purposes and THz spectroscopy for materials recognition and identification.

Natan S. Kopeika (SM'79–LS'10) was born in Baltimore, MD, in 1944. He received the B.Sc., M.Sc., and Ph.D. degrees in electrical engineering from the University of Pennsylvania, Philadelphia, in 1966, 1968, and 1972, respectively.

He and his family moved to Israel, and he began his career at Ben-Gurion University of the Negev, Beer-Sheva, Israel, in 1973. He Chaired the Department of Electrical and Computer Engineering for two terms (1989 to 1993), and was named Reuven and Francis Feinberg Professor of Electrooptics in 1994. He was the first Chairman of the new Department of Electrooptical Engineering, which grants graduate degrees in Electrooptical Engineering. He has published over 170 papers in international reviewed journals and well over 100 papers at various conferences. Areas of research include interactions of electromagnetic waves with plasmas, the optogalvanic effect, environmental effects on optoelectronic devices, imaging system theory, propagation of light through the atmosphere, imaging through the atmosphere, image processing and restoration from blur, imaging in the presence of motion and vibration, lidar, target acquisition, and image quality in general. He is the author of the textbook *A System Engineering Approach to Imaging* (SPIE, 1998) [first printing 1998, second printing 2000]. He is Topical Editor for Marcel Dekker for the topic "Atmospheric Optics" in their *Encyclopedia of Optical Engineering*.

Dr. Kopeika is a Fellow of The International Society for Optical Engineers (SPIE) and a Senior Member of IEEE. He was awarded the J. J. Thomson Prize by the IEE in 1999.

Yitzhak Yitzhaky received the B.S., M.S., and Ph.D. degrees in electrical and computer engineering from Ben-Gurion University, Beer-Sheva, Israel, in 1993, 1995, and 2000, respectively.

From 2000 to 2002, he was a Postdoctoral Research Fellow at the Schepens Eye Research Institute, Harvard Medical School, Boston, MA. Currently, he is with the Electro-Optics Unit at Ben-Gurion University. His research is mainly in the fields of image restoration, image enhancement and computer vision.

Alexander Belenky, photograph and biography not available at the time of publication.

Orly Yadid-Pecht, photograph and biography not available at the time of publication.